Effect of Surface Roughness on the Squeeze film lubrication of porous partial Journal Bearings with Micropolar fluids.

[1]Santosh Huggi
[1]Assistant Professor
[1]Department of Mathematics,
[1]Government First Grade College, Shahapur, Karnataka, INDIA
*Corresponding author e-mail: huggiss1979@gmail.com

Abstract: In this paper an attempt has been made to study the effect of surface roughness on the squeeze film lubrication of porous partial journal bearing with micropolar fluid. On the basis of Christensen's stochastic theory for the study of rough surfaces, the stochastic generalized Reynolds equation is derived for the micropolar fluids. Two types of one dimensional rough structures viz; longitudinal roughness pattern and the transverse roughness pattern are considered. It is assumed that, the roughness asperity heights are small as compared to the film thickness. The averaged film pressure distribution equation is solved numerically by using the conjugate gradient method. According to the results, the effect of micropolar fluid is to increase the film pressure, load carrying capacity and reduces the squeezing velocity. The effect of surface roughness on the squeeze film characteristics is dependent on the type of roughness structure.

Key words: Porous, Partial journal bearings, Squeeze films, Micropolar fluids, Surface roughness.

I. INTRODUCTION

Self-lubricating porous journal bearings are extensively used in industrial applications because of their long life without any external supply of lubricants. An extensive study of porous journal bearings has been made during the last few decades Cameron [1], Roulean [2], Wu [3], Bhatt [4] and Murthi [5-6]. These studies are confined to Newtonian lubricants. The pulsating or reciprocating loads on bearings and bearing surfaces are produced in several machine components. Due to this the oil film breaks down and relatively high friction and wear are to be expected. When the conditions are favorable an oil film is maintained between the contacting surfaces when the relative motion is momentarily zero. The load carrying phenomenon arises due to the fact that a viscous lubricant cannot be squeezed out instantaneously from between two matting surfaces due to the resistance of lubricants to extrusion, pressure build up and hence load is supported by the lubricant film. When the load is relived or reversed the lubricant film can recover its thickness before the next cycle if the bearing has been designed to permit this build up. Such phenomenon is observed in reciprocating machines in which the bearings are subjected to fluctuating dynamic loads. When the bearings are subjects to reciprocating loads the lubricants may become contaminated with dirt and metal particles then the lubricant behaves as a fluid suspension. The classical Newtonian theory will not predict the accurate flow behaviour of fluid suspensions specially when the clearance in the bearing is comparable with the average size of the lubricant additives. An experimental study of Henniker [7] suggests that an addition of 2% aluminimum napthenate to turbine oil produces a many fold increases in its effective viscosity in thin films. Several microcontinuum theories have been proposed to take into account of intrinsic motion of material constituents. The Eringen's [8] microcontinuum theory of micropolar fluid theory has gained considerable attention, as this theory has unique feature which is suitable for modeling a wide variety of fluid flow problems. The micropolar fluids are the subclass of micro fluids which include the effects of local rotating inertia couple stresses and inertial spin. Several investigators used the micropolar fluid theory for the study of several bearings systems.[9-12].

All the studies mentioned above have been made under the common assumption that the bearing surfaces are perfectly smooth. Even early attempts to develop a theory of friction recognized the fact that all practically prepared surfaces are rough on the microscopic scale. The aspect ratio and absolute height of the asperities and valleys observed under the microscope vary greatly depending on the material properties and on the method of surface preparation. Height of the surface roughness may range from 0.05 micrometer or less on polished surfaces to 10 micrometer on medium machined surfaces. Even the chemical degration of the lubricants leading to the contamination of lubricants is also a plausible reason for developing roughness on the bearing surfaces in some cases. The study of surface roughness on the bearing surfaces has attracted several researchers in the field of tribology during the last few decades. Several methods have been proposed to study the effects of surface roughness on the bearing performance. Due to the random structure of the surface roughness, a stochastic approach has been used to mathematically model the surface roughness Christensen [13] developed a stochastic model for the study of surface roughness on hydrodynamic lubrication of bearings and this theory formed the basis for the study of several investigators [14-18]. In all these studies it is assumed that the probability density function for the random variable characterizing the surface roughness is symmetric and has zero mean.

The aim of this paper is to study the effect of the surface roughness on the finite partial porous journal bearing with squeezing effect of micropolar fluids.

2. MATHEMATICAL FORMULATION OF THE PROBLEM

The physical configuration of the problem under consideration is shown in the figure 1. The journal of radius R approaches the porous bearing surface at a circumferential section, θ with velocity, $V\left(=\frac{\partial h}{\partial t}\right)$ The film thickness h is a function of θ and is given by

$$h = C + e\cos\theta \tag{1}$$

where 'C' is radial clearance and 'e' is the eccentricity of the journal centre. The lubricant in the film region and also in the porous region is assumed to be Eringen's [8] micropolar fluid.

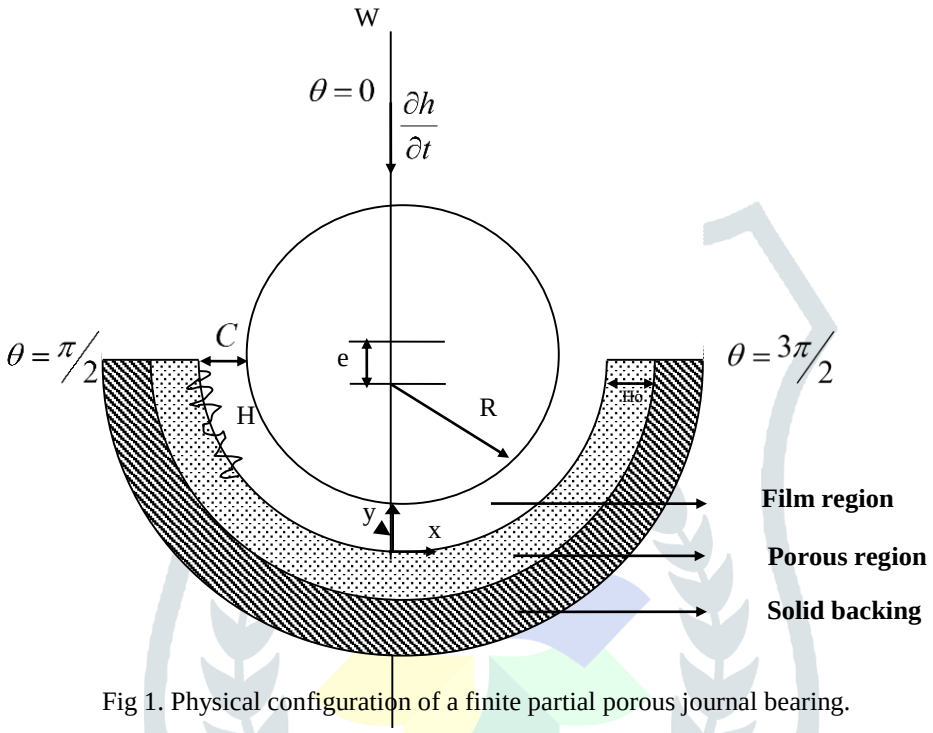

Fig 1. Physical configuration of a finite partial porous journal bearing.

The constitutive equations for micropolar fluids proposed by Eringen [8] simplify considerably under the usual assumptions of hydrodynamic lubrication. The resulting equations under steady–state conditions are

Conservation of linear momentum:

$$\left(\mu + \frac{\chi}{2}\right)\frac{\partial^2 u}{\partial y^2} + \chi\frac{\partial v_3}{\partial y} - \frac{\partial p}{\partial x} = 0\,, \tag{2}$$

$$\left(\mu + \frac{\chi}{2}\right)\frac{\partial^2 w}{\partial y^2} - \chi\frac{\partial v_1}{\partial y} - \frac{\partial p}{\partial y} = 0\,. \tag{3}$$

Conservation of angular momentum:

$$\gamma\frac{\partial^2 v_1}{\partial y^2} - 2\chi v_1 + \chi\frac{\partial w}{\partial y} = 0\,, \tag{4}$$

$$\gamma\frac{\partial^2 v_3}{\partial y^2} - 2\chi v_3 - \chi\frac{\partial u}{\partial y} = 0\,. \tag{5}$$

Conservation of mass:

$$\frac{\partial u}{\partial x} + \frac{\partial v}{\partial y} + \frac{\partial w}{\partial z} = 0 \tag{6}$$

Where (u, v, w) are the velocity components of the lubricant in the x, y and z directions, respectively, and (v_1, v_2, v_3) are micro rotational velocity components, χ is the spin viscosity and γ is the viscosity coefficient for micropolar fluids and μ is the Newtonian viscosity coefficient.

The flow of micropolar lubricants in a porous matrix governed by the modified Darcy law, which account for the polar effects is given by [20]

$$\vec{q}^{*}=\frac{-k}{(\mu+\chi)}\nabla p^{*} \tag{7}$$

Where $\vec{q}^{*}=\left(u^{*},v^{*},w^{*}\right)$ is the modified Darcy velocity vector, with

$$u^{*}=\frac{-k}{(\mu+\chi)}\frac{\partial p^{*}}{\partial x}\quad,\quad v^{*}=\frac{-k}{(\mu+\chi)}\frac{\partial p^{*}}{\partial y}\quad,\quad w^{*}=\frac{-k}{(\mu+\chi)}\frac{\partial p^{*}}{\partial z} \tag{8}$$

k is the permeability of the porous matrix and p^{*} is the pressure in the porous region.

Due to continuity of fluid in the porous matrix, p^{*} satisfies the Laplace Equation.

$$\frac{\partial^{2}p^{*}}{\partial x^{2}}+\frac{\partial^{2}p^{*}}{\partial y^{2}}+\frac{\partial^{2}p^{*}}{\partial z^{2}}=0 \tag{9}$$

The relevant boundary conditions are

(a) at the bearing surface $(y=0)$

$$u=0,\ v=v^{*},\ w=0 \tag{10a}$$

$$v_{1}=0\ ,\ v_{3}=0 \tag{10b}$$

(b) at the journal surface $(y=H)$

$$u=0,v=\frac{\partial H}{\partial t},\ w=0 \tag{11a}$$

$$v_{1}=0\ ,\ v_{3}=0 \tag{11b}$$

3 SOLUTION OF THE PROBLEM

The generalized Reynolds equation is given by [21]

$$\frac{\partial}{\partial x}\left[\left(f\left(N,l,H\right)+\frac{12\mu k H_{0}}{(\mu+\chi)}\right)\frac{\partial p}{\partial x}\right]+\frac{\partial}{\partial z}\left[\left(f\left(N,l,H\right)+\frac{12\mu k H_{0}}{(\mu+\chi)}\right)\frac{\partial p}{\partial z}\right]=12\mu\frac{\partial H}{\partial t} \tag{12}$$

Where

$$f\left(N,l,H\right)=H^{3}+12l^{2}H-6NlH^{2}\coth\left(\frac{NH}{2l}\right),\qquad \frac{\partial H}{\partial t}=C\frac{\partial\varepsilon}{\partial t}\cos\theta\ .$$

Let $f\left(h_{s}\right)$ be the probability density function of the stochastic film thickness h_{s} taking the stochastic average of equation (12) with respect to $f\left(h_{s}\right)$, we obtain

$$\frac{\partial}{\partial x}\left\{E\left[f\left(N,l,H\right)+12\psi\left(\frac{1-N^{2}}{1+N^{2}}\right)\right]\frac{\partial E(p)}{\partial\theta}\right\}+\left(\frac{1}{4\lambda^{2}}\right)\frac{\partial}{\partial z}\left\{E\left[f\left(N,l,H\right)+12\psi\left(\frac{1-N^{2}}{1+N^{2}}\right)\right]\frac{\partial E(p)}{\partial z}\right\}=12\mu\frac{\partial E(H)}{\partial t} \tag{13}$$

Where $$E(\bullet)=\int_{-\infty}^{\infty}(\bullet)f\left(h_{s}\right)dh_{s} \tag{14}$$

In accordance with Christensen (1970), we assume that

$$f\left(h_{s}\right)=\begin{cases}\dfrac{35}{32c^{7}}\left(c^{2}-h_{s}^{\,2}\right)^{3}, & -c\le h_{s}\le c\\ 0 & elsewhere\end{cases} \tag{15}$$

Where $\sigma=c/3$ is the standard deviation.

Introducing the non-dimensional scheme into equation (13)

$$\theta=\frac{x}{R}\ ,\ \bar{z}=\frac{z}{L}\ ,\ \bar{l}=\frac{l}{C}\ ,\ \bar{H}=\frac{H}{C}=\bar{h}+\bar{h}_{s},\ \bar{h}=\frac{\bar{h}}{C}=1+\varepsilon\cos\theta,\ \bar{h}_{s}=\frac{h_{s}}{C}\ \ \bar{k}=\frac{k}{C^{2}}\ ,\qquad \bar{H}_{0}=\frac{H_{0}}{C}\ ,$$

$$\bar{p}=\frac{E(p)C^{2}}{\mu R^{2}\left(\frac{d\varepsilon}{dt}\right)}\ ,\ \psi=\frac{kH_{0}}{C^{3}}\ ,\ N=\left(\frac{\chi}{\chi+2\mu}\right)^{\frac{1}{2}}\ \ \lambda=\frac{L}{2R},\ \bar{c}=\frac{c}{C},\ \bar{x}=\frac{x}{R},$$

Into equation (13), we get the modified stochastic Reynolds type equation (13) can be written in a non- dimensional form as

$$\frac{\partial}{\partial \bar{x}}\left\{\left[E\left[\bar{f}\left(N,\bar{l},\bar{H}\right)\right]+12\psi\left(\frac{1-N^2}{1+N^2}\right)\right]\frac{\partial \bar{p}}{\partial \bar{x}}\right\}+\left(\frac{1}{4\lambda^2}\right)\frac{\partial}{\partial \bar{z}}\left\{\left[E\left[\bar{f}\left(N,\bar{l},\bar{H}\right)\right]+12\psi\left(\frac{1-N^2}{1+N^2}\right)\right]\frac{\partial \bar{p}}{\partial \bar{z}}\right\}=12\cos\theta$$

(16)

where $\bar{f}\left(N,\bar{l},\bar{H}\right)=\bar{H}^3+12\bar{l}^2\bar{H}-6N\bar{l}\bar{H}^2\coth\left(\frac{N\bar{H}}{2\bar{l}}\right)$.

the left-hand side of the stochastic Reynolds equation (16) will depend upon the structures of surface roughness and the following two types of directional structures are of special theoretical interest.

Longitudinal Roughness

For the longitudinal model, the roughness is assumed to have the form of long narrow ridge and valleys running in the x-direction. Therefore the lubricant film thickness can be expressed as

$$\bar{H}=\bar{h}+\bar{h}_s(z,\xi) \tag{17}$$

And the Reynolds-type equation (16) can be reduced to

$$\frac{\partial}{\partial \bar{x}}\left\{\left[E\left[\bar{f}\left(N,\bar{l},\bar{H}\right)\right]+12\psi\left(\frac{1-N^2}{1+N^2}\right)\right]\frac{\partial \bar{p}}{\partial \bar{x}}\right\}+\left(\frac{1}{4\lambda^2}\right)\frac{\partial}{\partial \bar{z}}\left\{\left[\frac{1}{E\left[\bar{f}\left(N,\bar{l},\bar{H}\right)\right]}+12\psi\left(\frac{1-N^2}{1+N^2}\right)\right]\frac{\partial \bar{p}}{\partial \bar{z}}\right\}=12\cos\theta \tag{18}$$

Transverse Roughness

For the transverse model, the roughness is assumed to have the form of long narrow ridge and valley running in the z-direction. Therefore the lubricant film thickness can be expressed as

$$\bar{H}=\bar{h}+\bar{h}_s(\theta,\xi) \tag{19}$$

And the Reynolds-type equation (16) can be reduced to

$$\frac{\partial}{\partial \bar{x}}\left\{\left[\frac{1}{E\left[\bar{f}\left(N,\bar{l},\bar{H}\right)\right]}+12\psi\left(\frac{1-N^2}{1+N^2}\right)\right]\frac{\partial \bar{p}}{\partial \bar{x}}\right\}+\left(\frac{1}{4\lambda^2}\right)\frac{\partial}{\partial \bar{z}}\left\{\left[E\left[\bar{f}\left(N,\bar{l},\bar{H}\right)\right]+12\psi\left(\frac{1-N^2}{1+N^2}\right)\right]\frac{\partial \bar{p}}{\partial \bar{z}}\right\}=12\cos\theta \tag{20}$$

After simplication, the modified Reynolds equations for longitudinal and transverse types of directional structure can be expressed as

$$\frac{\partial}{\partial \bar{x}}\left\{\alpha\left(N,\bar{l},\bar{H}\right)\frac{\partial \bar{p}}{\partial \bar{x}}\right\}+\left(\frac{1}{4\lambda^2}\right)\frac{\partial}{\partial \bar{z}}\left\{\beta\left(N,\bar{l},\bar{H}\right)\frac{\partial \bar{p}}{\partial \bar{z}}\right\}=12\cos\theta \tag{21}$$

Where

$$\alpha\left(N,\bar{l},\bar{H}\right)=\begin{cases}E\left[\bar{f}\left(N,\bar{l},\bar{H}\right)\right]+12\psi\left(\frac{1-N^2}{1+N^2}\right) & longitudinal\ roughness\\ \frac{1}{E\left[\bar{f}\left(N,\bar{l},\bar{H}\right)\right]}+12\psi\left(\frac{1-N^2}{1+N^2}\right) & transverse\ roughness\end{cases}$$

$$\beta\left(N,\bar{l},\bar{H}\right)=\begin{cases}\frac{1}{E\left[\bar{f}\left(N,\bar{l},\bar{H}\right)\right]}+12\psi\left(\frac{1-N^2}{1+N^2}\right) & longitudinal\ roughness\\ E\left[\bar{f}\left(N,\bar{l},\bar{H}\right)\right]+12\psi\left(\frac{1-N^2}{1+N^2}\right) & transverse\ roughness\end{cases}$$

$$E\left[\bar{f}\left(N,\bar{l},\bar{H}\right)\right]=\bar{H}^3+\frac{\bar{H}c^2}{3}+12\bar{H}\bar{l}^2-6N\bar{l}\left(\bar{H}^2+\frac{c^2}{9}\right)\times g$$

$$g=\frac{35}{32c^7}\int_{-c}^{c}\left(c^2-\bar{h}_s^{\,2}\right)^3\times\left(\frac{1}{\tanh\left(\frac{N\bar{H}}{2\bar{l}}\right)}\right)d\bar{h}_s$$

$$\frac{1}{E\left[\bar{f}\left(N,\bar{l},\bar{H}\right)\right]}=\frac{35}{32c^7}\int_{-c}^{c}\frac{\left(c^2-\bar{h}_s^{\,2}\right)^3}{\bar{H}^3+12\bar{H}\bar{l}^{\,2}-6N\bar{l}\bar{H}^2\left(\dfrac{1}{\tanh\left(\dfrac{N\bar{H}}{2\bar{l}}\right)}\right)}\times d\bar{h}_s$$

In order to solve the stochastic generalized Reynolds equation (21) to obtain the film pressure distribution of the journal bearing system. The Reynolds boundary conditions are used

$$\bar{p}=0 \quad \text{at} \quad \theta=\frac{\pi}{2},\frac{3\pi}{2} \quad \text{and} \quad \bar{p}=0 \quad \text{at} \quad \bar{z}=\pm\frac{1}{2} \tag{22}$$

Numerical formulation

Since the modified Reynolds equation (21) is too complicated to be solved analytically , a finite difference scheme is adopted. First, the film domain under consideration is divided by the grid spacing shown in figure 2. then the mesh for the film extent is constructed. To avoid the divergence of the finite difference scheme. The conservative form of finite increment formats is applied, in this case, the terms of equation (21) are given by

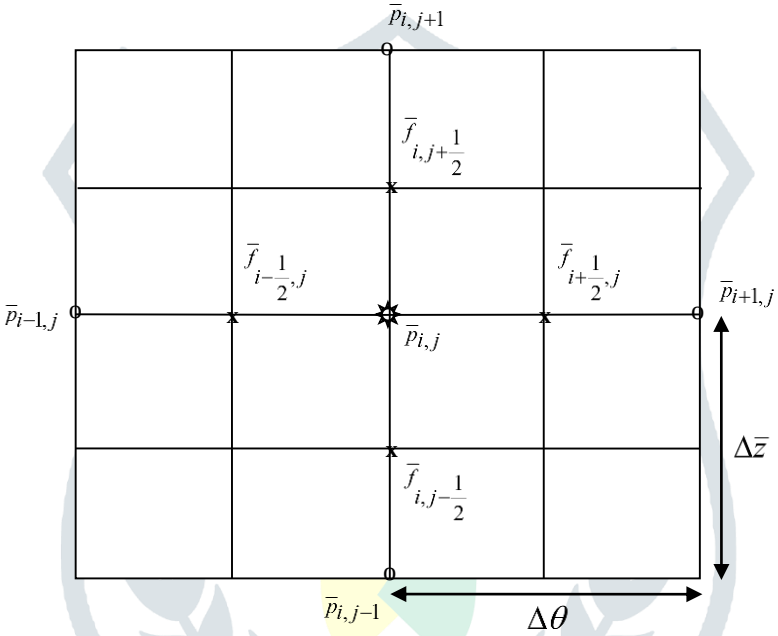

Fig. 2. Grid point notation for the film element

$$\frac{\partial}{\partial\theta}\left[\alpha\left(N,\bar{l},\bar{H}\right)\frac{\partial\bar{P}}{\partial\theta}\right]=$$

$$\frac{1}{\Delta\theta}\left[\left(\bar{f}_{i+\frac{1}{2},j}+12\psi\left(\frac{1-N^2}{1+N^2}\right)\right)\left(\frac{\bar{P}_{i+1,j}-\bar{P}_{i,j}}{\Delta\theta}\right)-\left(\bar{f}_{i-\frac{1}{2},j}+12\psi\left(\frac{1-N^2}{1+N^2}\right)\right)\left(\frac{\bar{P}_{i,j}-\bar{P}_{i-1,j}}{\Delta\theta}\right)\right]$$

$$\frac{1}{4\lambda^2}\times\frac{\partial}{\partial\bar{z}}\left[\beta\left(N,\bar{l},\bar{H}\right)\frac{\partial\bar{P}}{\partial\bar{z}}\right]=$$

$$\frac{1}{4\lambda^2}\times\frac{1}{\Delta\bar{z}}\left[\left(\bar{f}_{i,j+\frac{1}{2}}+12\psi\left(\frac{1-N^2}{1+N^2}\right)\right)\left(\frac{\bar{P}_{i,j+1}-\bar{P}_{i,j}}{\Delta\bar{z}}\right)-\left(\bar{f}_{i,j-\frac{1}{2}}+12\psi\left(\frac{1-N^2}{1+N^2}\right)\right)\left(\frac{\bar{P}_{i,j}-\bar{P}_{i,j-1}}{\Delta\bar{z}}\right)\right]$$

After the Substitution for the above finite difference forms, the modified Reynolds equation leads to

$$\bar{P}_{i,j}=C_1\bar{P}_{i+1,j}+C_2\bar{P}_{i-1,j}+C_3\bar{P}_{i,j+1}+C_4\bar{P}_{i,j-1}+C_5 \tag{23}$$

where

$$C_0 = 4\lambda^2 r^2 \left\{ \left(\bar{f}_{i+\frac{1}{2},j} + 12\psi \left(\frac{1-N^2}{1+N^2} \right) \right) + \left(\bar{f}_{i-\frac{1}{2},j} + 12\psi \left(\frac{1-N^2}{1+N^2} \right) \right) \right\} + \left(\bar{f}_{i,j+\frac{1}{2}} + 12\psi \left(\frac{1-N^2}{1+N^2} \right) \right) + \left(\bar{f}_{i,j-\frac{1}{2}} + 12\psi \left(\frac{1-N^2}{1+N^2} \right) \right) \tag{23.a}$$

$$C_1 = 4\lambda^2 r^2 \left(\bar{f}_{i+\frac{1}{2},j} + 12\psi \left(\frac{1-N^2}{1+N^2} \right) \right) \Big/ C_0 , \tag{23.b}$$

$$C_2 = 4\lambda^2 r^2 \left(\bar{f}_{i-\frac{1}{2},j} + 12\psi \left(\frac{1-N^2}{1+N^2} \right) \right) \Big/ C_0 , \tag{23.c}$$

$$C_3 = \left(\bar{f}_{i,j+\frac{1}{2}} + 12\psi \left(\frac{1-N^2}{1+N^2} \right) \right) \Big/ C_0 , \tag{23.d}$$

$$C_4 = \left(\bar{f}_{i,j-\frac{1}{2}} + 12\psi \left(\frac{1-N^2}{1+N^2} \right) \right) \Big/ C_0 , \tag{23.e}$$

$$C_5 = -48\lambda^2 \cos\theta_i \Delta\bar{z}^2 \Big/ C_0 , \; r = \frac{\Delta\bar{z}}{\Delta\theta} . \tag{23.f}$$

The pressure, $\bar{p}$ is calculated by using the numerical method with grid spacing of $\Delta\theta = 9^0$ and $\Delta\bar{z} = 0.05$.

The load carrying capacity of the bearing, W generated by the film pressure is obtained by

$$E(W) = -LR \int_{\theta=\pi/2}^{\theta=3\pi/2} \int_{z=-1/2}^{z=1/2} E(p) \cos\theta \, d\theta . dz \tag{24}$$

The non-dimensional load carrying capacity, $\bar{W}$ of the 180^0 porous partial journal bearing is obtained in the form

$$\bar{W} = \frac{E(W)C^2}{\mu LR^3 \left(\frac{d\varepsilon}{dt} \right)} = -\int_{\theta=\pi/2}^{\theta=3\pi/2} \int_{\bar{z}=-1/2}^{\bar{z}=1/2} \bar{P} \cos\theta_i d\theta . d\bar{z} \tag{25}$$

$$\approx \sum_{i=0}^{M} \sum_{j=0}^{N} \bar{P}_{i,j} \cos\theta_i \Delta\theta . \Delta\bar{z} = g\left(\varepsilon, \bar{l}, N, \psi\right)$$

where M+1 and N+1 are the grid point numbers in the x and z directions respectively.

Time-height relation is calculated by considering the time taken by the journal center to move from $\varepsilon = 0$ to $\varepsilon = \varepsilon_1$ can be obtained from equation (25)

$$\frac{d\varepsilon}{d\tau} = \frac{1}{g\left(\varepsilon, \bar{l}, N, \psi\right)} \tag{26}$$

Where $\tau = \dfrac{WC^2}{\mu LR^3} t$ is the non-dimensional response time.

The first order non-linear differential equation (26) is solved numerically by using the fourth order Runge-Kutta method with the initial conditions $\varepsilon = 0$ to $\tau = 0$.

4 RESULTS AND DISCUSSIONS

The effect of surface roughness pattern on the squeeze film characteristics of a finite partial journal bearings lubricated with micropolar fluids are obtained for different values of various non-dimensional parameters such as coupling number, $N\left(= \dfrac{\chi}{\chi + 2\mu} \right)^{1/2}$ the parameter, $\bar{l}\left(= l/C \right)$ characterizes the interaction of the bearing geometry with the lubricant

properties. In the limiting case as $\bar{l} \to 0$ the effect of microstructures becomes negligible. The effect of permeability is observed through the non-dimensional permeability parameter, $\psi \left(= \frac{kH_0}{C^3} \right)$ and it is to be noted that as $\psi \to 0$ the problem reduces to the corresponding solid case.

The effect surface roughness is characterized by the roughness parameter $\bar{c} \left(= c/C \right)$ and it is to be noted that as $\bar{c} \to 0$ the problem reduces to the corresponding smooth case and as $\bar{l}, N \to 0$ it reduces to the corresponding Newtonian case.

4.1 SQUEEZE FILM PRESSURE

The variation of non-dimensional squeeze film pressure $\bar{p}$ for different values of $\bar{l}$ as a function is shown in fig.3 with the parameter values of $N = 0.8, \lambda = 1.5, \varepsilon = 0.2, \bar{c} = 0.2$ and $\psi = 0.01$ for both types of roughness patterns. It is observed that, the effect of $\bar{l}$ is to increases $\bar{p}$ in either cases as compared to Newtonian case. Further the increase in $\bar{p}$ is more pronounced for the longitudinal roughness pattern as compared to the transverse roughness pattern.

The variation of non-dimensional film pressure $\bar{p}$, for different values of $\bar{c}$ roughness parameter $\bar{c}$ as a function is shown in fig.4. with the parameter values of $\bar{l} = 0.2, N = 0.8, \lambda = 3.0, \varepsilon = 0.6$ and $\psi = 0.01$, for both types of roughness patterns. It is observed that, the effect of longitudinal (transverse) roughness pattern is to increases(decreases) as compared to the corresponding smooth case.

4.2 LOAD CARRYING CAPACITY

The variation of non-dimensional load carrying capacity $\bar{W}$ with eccentricity ratio parameter, ε for different values of $\bar{l}$ with $N = 0.8, \psi = 0.01, \bar{c} = 0.2 \; and \; \lambda = 1.5$ is shown in the fig 5. It is observed that, $\bar{W}$ increases for the increasing values of ε increases and this increase is more accentuated for larger values of $\bar{l}$ for both the types of roughness patterns. Further the increases in $\bar{W}$ is more pronounced for the longitudinal roughness pattern as compared to the transverse roughness pattern. The variation of non-dimensional load carrying capacity $\bar{W}$ with eccentricity ratio parameter, ε for different values of N with $\bar{l} = 0.8, \psi = 0.1, \bar{c} = 0.2 \; and \; \lambda = 2.5$ is shown in the fig 6. It is observed that, $\bar{W}$ increases for the increasing values of N for both the types of roughness patterns. Further the increases in $\bar{W}$ is more pronounced for the longitudinal roughness pattern as compared to the transverse roughness pattern. The variation of non-dimensional load carrying capacity $\bar{W}$ with eccentricity ratio parameter, ε as a function of roughness parameter $\bar{c}$ with $N = 0.8, \bar{l} = 0.2, \psi = 0.01 \; and \; \lambda = 3.0$ is depicted in the figure 7. it is observed that, the effect of longitudinal (transverse) roughness pattern is to increases (decreases) $\bar{W}$ as compared to the corresponding smooth case.

4.3 MINIMUM SQUEEZE FILM HEIGHT

The response time of the squeeze film is one of the significant factor in the design of bearings. The response time is the time that will elapse for a squeeze film reduces to some minimum permissible height.

The variation of the non-dimensional minimum film height $\bar{h}_0 \left(= 1 - \varepsilon \right)$ with the non-dimensional time τ as a function of $\bar{l}$ with $N = 0.8, \psi = 0.01, \bar{c} = 0.2 \; and \; \lambda = 1.5$ is shown in the figure.8. It is observed that, the response time increases for increasing values of $\bar{l}$ for both the types of roughness patterns, hence the pressure of the mocrostructures in the lubricant the squeeze film time as compared to that of the Newtonian lubricants. This result can be attributed to the increased load carrying capacity for the micropolar fluids as compared to the corresponding Newtonian lubricants. The variation of the non-dimensional minimum squeeze film height, $\bar{h}_0$ with τ as a function of the coupling number N with $\bar{l} = 0.8, \psi = 0.1, c = 0.2$ and $\lambda = 2.5$ is shown in the figure.9. It is observed that, the response time increases for increasing values of N for both the types of roughness patterns. The variation of the non-dimensional minimum squeeze film height, $\bar{h}_0$ with τ as a function of non-dimensional roughness parameter, $\bar{c}$ with $N = 0.8, \bar{l} = 0.2, \psi = 0.01$ and $\lambda = 3.0$ .is depicted in the figure 10. It is interesting to note that the effect of $\bar{c}$ is to increases (decreases) the response time of the squeeze film for the longitudinal (transverse) roughness pattern as compared to the corresponding smooth case ($\bar{c} = 0.0$).

CONCLUSIONS

On the basis of Eringen's [8] micropolar fluid theory and Christensen stochastic theory for rough surfaces this paper predicts the effect of micropolar on the squeeze film characteristics of finite partial rough porous journal bearings. The following conclusion can be drawn on the basis of the results and discussion.

1) The presence of the microstrucutre additives in the lubricants enhances the load carrying capacity and squeeze film time as compared to the corresponding Newtonian case.
2) The Christensen surface roughness longitudinal (Transverse) pattern on the finite porous partial journal bearings increases (decreases) the load carrying capacity and the squeeze film time as compared to the corresponding smooth case.
3) The presence of the porous facing on the bearing surface reduces the load carrying capacity and response time.

NOMENCLATURE

C radial clearance
c roughness parameter
$\bar{c}$ non-dimensional parameter (= *c/C)*
e eccentricity
E expectancy operator
h mean film thickness $\left(h=C+e\cos\theta\right)$
$\bar{h}$ non-dimensional film thickness (= *h/C*)
H film thickness $\left(=h+h_s\right)$
h_s stochastic film thickness
$\bar{h}_0$ minimum film height
H_0 porous layer thickness
k permeability of the porous matrix
l characteristic length of the polar suspension $\left(=\left(\frac{\gamma}{4\mu}\right)^{\frac{1}{2}}\right)$
$\bar{l}$ non-dimensional form of l (= *l/C)*
L bearing length
N coupling number $\left(=\left(\frac{\chi}{\chi+2\mu}\right)^{\frac{1}{2}}\right)$
p lubricant pressure
σ standard deviation
R radius of the journal
$\bar{p}$ non-dimensional pressure $\left(=\frac{E(p)C^2}{\mu R^2\left(\frac{d\varepsilon}{dt}\right)}\right)$
t time
u,v,w components of fluid velocity in *x*, *y* and *z* directions, respectively
v_1,v_2,v_3 microrotational velocity components in the *x* , *y* and *z* directions
r,θ,z cylindrical co-ordinates
V squeeze velocity, $\frac{\partial H}{\partial t}\left(=C\frac{\partial\varepsilon}{\partial t}\cos\theta\right)$
W load carrying capacity
$\bar{W}$ non-dimensional load carrying capacity $\left(=\frac{E(W)C^2}{\mu L R^3\left(\frac{d\varepsilon}{dt}\right)}\right)$
x,y,z Cartesian co-ordinates

ε eccentricity ratio (= e/C)

χ spin viscosity

γ viscosity co-efficient for micropolar fluids

μ viscosity co-efficient

τ dimensionless response time

ψ permeability parameter (= kH_0/C^3)

θ circumferential co-ordinate (= x/R)

λ length to diameter ratio (=$L/2R$)

Δ gradient operator

REFERENCE

[1] Cameron, A., Morgan, V. T. and Stainsby A.E. Critical conditions for hydrodynamics lubrication of porous metal bearings. *Proc. Inst. Mech. Engg, London*,1962,Vol. 176, pp 761-770.

[2] Rouleau W. T., Hydrodynamic lubrication of narrow press fitted porous metal bearings, J. Basic Eng., 1963, Vol.85. pp123-128.

[3] Wu. H., An analysis of squeeze film between porous rectangular plates ASME. J. Lubr. Techonl. 1972,Vol.94, pp. 64-68.

[4] Bhatt M.V., Hydrodynamic Lubrication of porous composite slide bearing . Japanese Journal of Applied physics. 1978. Vol.17. No.3., pp. 479-481.

[5] Murti P.R.K., Hydrodynamic lubrication of finite bearings. *Wear*, 1972, Vol.19, pp. 113-115.

[6] Murthi P.R.K., Effect of slip flow in narrow porous bearings with arbitary wall thickness. J. Applied Mech.1972, Vol. 2(2), pp. 518-523.

[7] Henniker J.C., The Depth of the surface zone of a liquid. Rev. Mod. Phys, 949, Vol 21, pp.322-

[8] Eringen A. C., Theory of micropolar fluids, *J. Math and Mech., 1966,Vol.16. pp. 1-18.*

[9] Allen S.J and Kline K.A., Lubrication theory for microfluids. J. Appl.Mech. Tran, ASME, 1971, Vol.38, pp. 646-650.

[10] Prakash J. and Sinha P., Cyclic Squeeze films in micropolar fluid lubricated journal bearings, *Trans. ASME. J. Lubr. Technol*. 1975, Vol.98, p.412-417.

[11] Prakash J. and Sinha P., Squeeze film theory for micropolar fluids, *J. Lubr. Technol*. 1976. p.139-144.

[12] Zaheeruddin K.H and Isa .M., One dimensional porous journal bearing lubrication with micropolar fluid. *Wear*, 1980, Vol. 83, pp257-270.

[13] Christensen H., Stochastic models for hydrodynamic lubrication of rough surfaces. Proceedings of the institute mechanical engineers, part-I, 1970.Vol.184, p.1013-1026.

[14] Prakash J and Tiwari K., Lubrication of a porous bearing with surface corrugations, ASME, Journal of Lubrication Technology. 1982a, Vol.104, p.127-134.

[15] Prakash J and Tiwari K., An analysis of squeeze film between porous rectangular plates including the surface roughness effects. Journal of Mechanical Engineering Science. 1982b, Vol.24, No-1, p.45-49.

[16] Prakash J and Tiwari K., Effects of surface roughness on the squeeze film between rotating porous annular discs. Journal of Mechanical Engineering Science. 1982c, Vol.24, No-3, p.155-161.

[17] Gururajan K and Prakash J., surface roughness effects in infinitely long porous journal bearings. ASME Journal of Tribology, 1999, Vol. 121, p. 139-147.

[18] Gururajan K and Prakash J., Effects of surface roughness in a narrow porous journal bearing, ASME Journal of Tribology, 2000, Vol. 122, p. 472-475.

[19] Naduvinamani N. B and Kashinath B., Surface roughness effects on the stastic and dynamic behaviour of squeeze film lubrication of short journal bearings with micropolar fluids. Proc. Imech. Engg. J. Engg. Tribology [part J], 2008, Vol. 222., pp.121-131.

[20] Naduvinamani N. B and Santosh S. On the squeeze film lubrication of rough short porous partial journal bearings with micropolar fluid. *J. Engg. Tribol.* 2009, (in press)

[21] Naduvinamani N. B and Santosh S. Huggi., micropolar fluid squeeze film lubrication of short partial porous journal bearing, *J. Engg. Tribol.* 2009, Vol.223, pp. 1179-1185.

FIGURE CAPTIONS

Fig 1: Physical configuration of a finite partial porous journal bearing.

Fig 2: Grid point notation for the film element.

Fig 3: Non-dimensional film pressure $\bar{p}$ for different values of $\bar{l}$ with $N=0.8, \psi=0.01, \lambda=1.5, \varepsilon=0.2$ and $\bar{c}=0.2$.

Fig 4: Non-dimensional film pressure $\bar{p}$ for different values of $\bar{c}$ with $\bar{l}=0.2, N=0.8, \lambda=3.0, \varepsilon=0.6$ and $\psi=0.01$.

Fig 5: Variation of non-dimensional load $\bar{W}$ with ε for different values of $\bar{l}$ with $N=0.8, \psi=0.01, \bar{c}=0.2$ and $\lambda=1.5$.

Fig 6: Variation of non-dimensional load $\bar{W}$ with ε for different values of N with $\bar{l}=0.8, \psi=0.1, \bar{c}=0.2$ and $\lambda=2.5$.

Fig 7: Variation of non-dimensional load $\bar{W}$ with ε for different values of $\bar{c}$ with $\bar{l}=0.2, N=0.8, \psi=0.01$ and $\lambda=3.0$.

Fig 8: Variation of non-dimensional minimum film height $\bar{h}_0$ verses τ for different values of $\bar{l}$ with $N=0.8, \psi=0.01, \bar{c}=0.2$ and $\lambda=1.5$.

Fig 9: Variation of non-dimensional minimum film height $\bar{h}_0$ verses τ for different values of N with $\bar{l}=0.8, \psi=0.1, \bar{c}=0.2$ and $\lambda=2.5$.

Fig 10: Variation of non-dimensional minimum film height $\bar{h}_0$ verses τ for different values of $\bar{c}$ with $\bar{l}=0.2, N=0.8, \psi=0.01$ and $\lambda=3.0$.

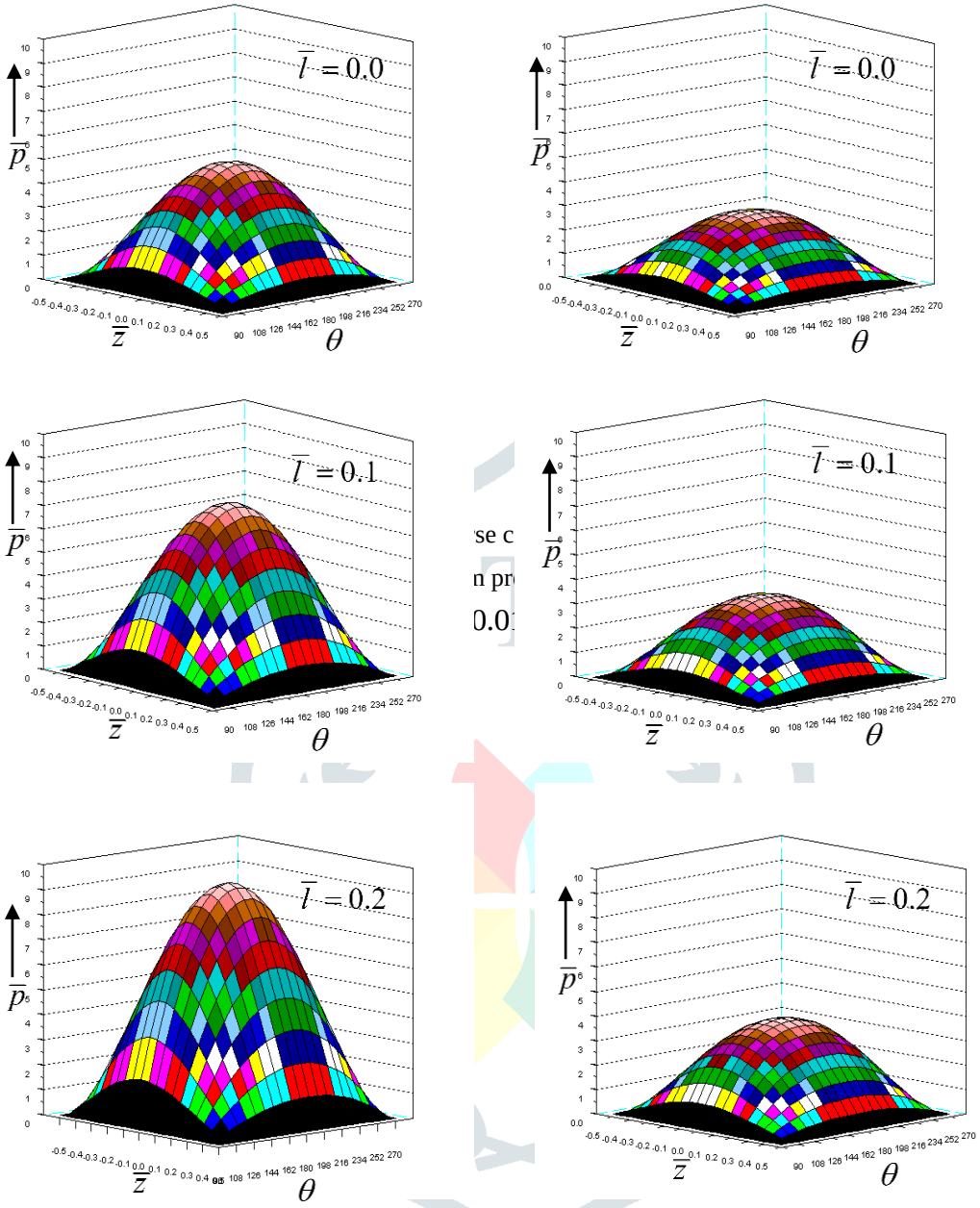

Fig 3: Non-dimensional film pressure $\bar{p}$ for different values of $\bar{l}$ with $N = 0.8, \psi = 0.01, \lambda = 1.5, \varepsilon = 0.2$ and $\bar{c} = 0.2$.

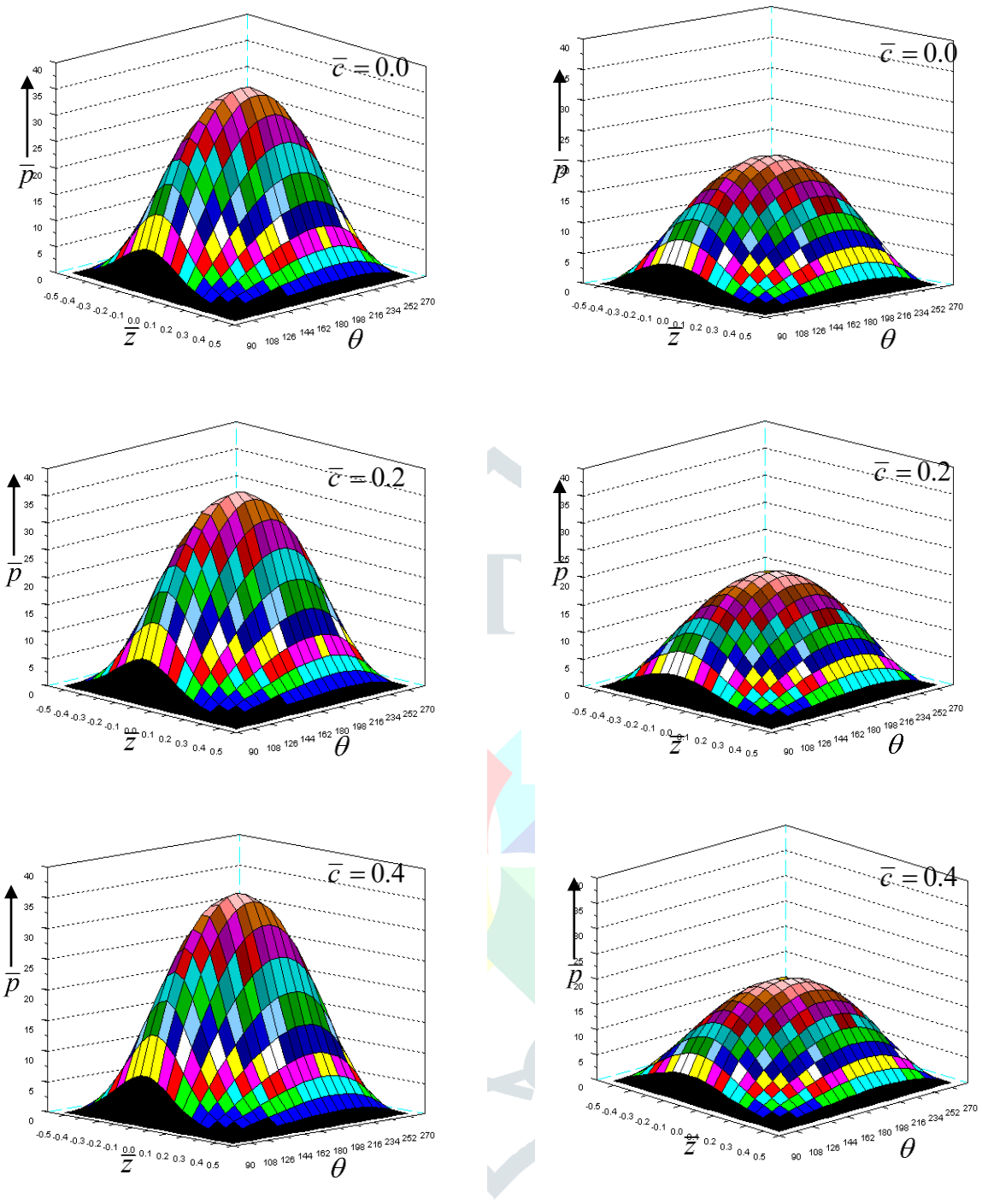

Fig.4. Non-dimensional film pressure $\bar{p}$ for different values of $\bar{c}$ with

$\bar{l} = 0.2,\ N = 0.8, \lambda = 3.0,\ \varepsilon = 0.6\, and\, \psi = 0.01.$

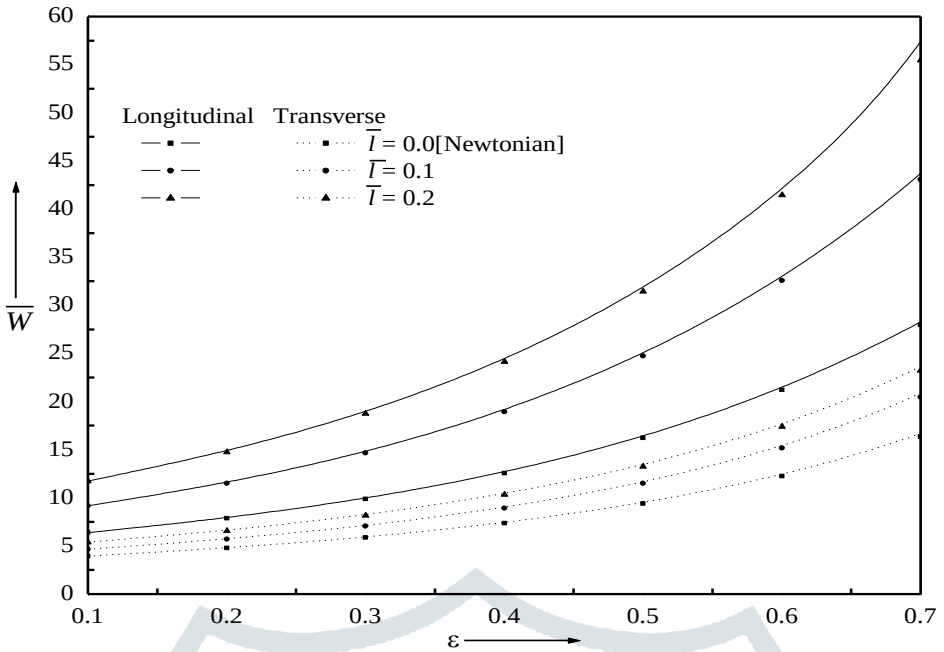

Fig.5. Variation of non-dimensional load $\bar{W}$ with ε for different values of $\bar{l}$ with N = 0.8, ψ = 0.01, $\bar{c}$ = 0.2 and λ = 1.5

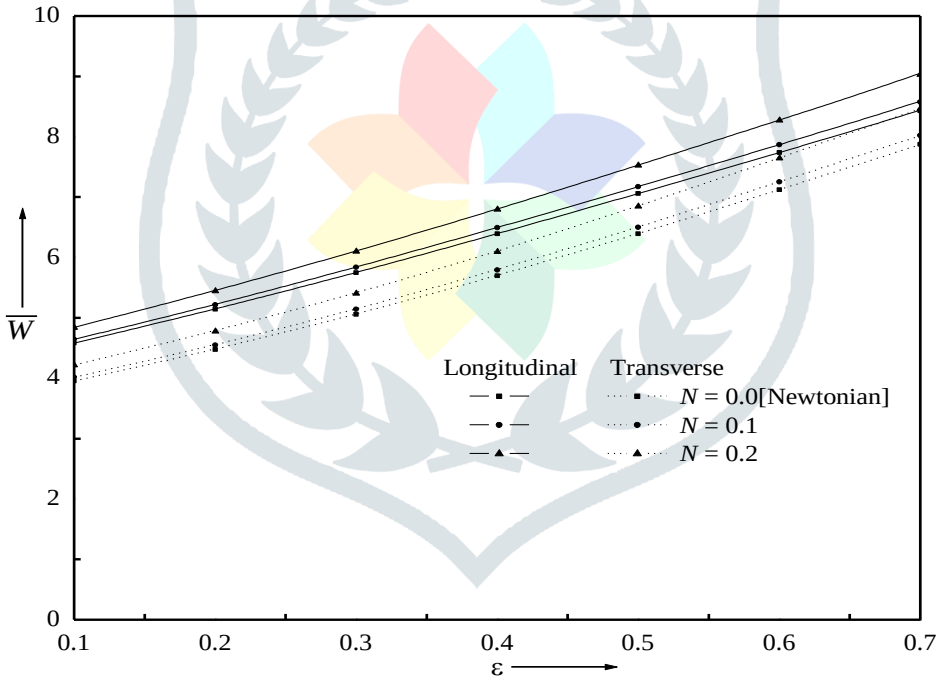

Fig.6. Variation of non-dimensional load $\bar{W}$ with ε for different values of N with $\bar{l}$ = 0.8, ψ = 0.1, $\bar{c}$ = 0.2 and λ = 2.5

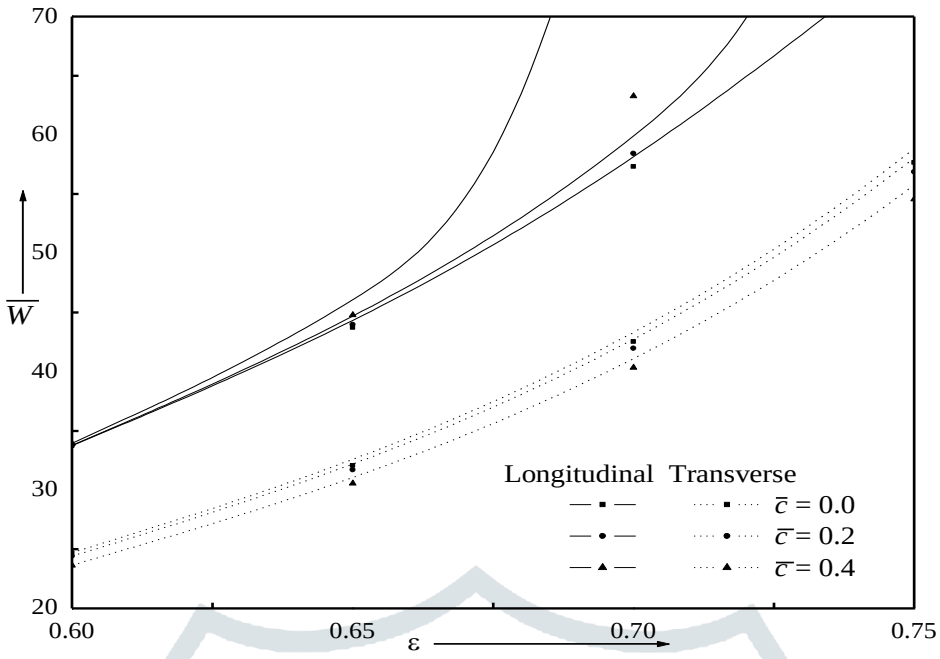

Fig.7. Variation of non-dimensional load $\overline{W}$ with ε for different values of $\bar{c}$ with N = 0.8, $\bar{l}$ = 0.2, ψ = 0.01 and λ = 3.0

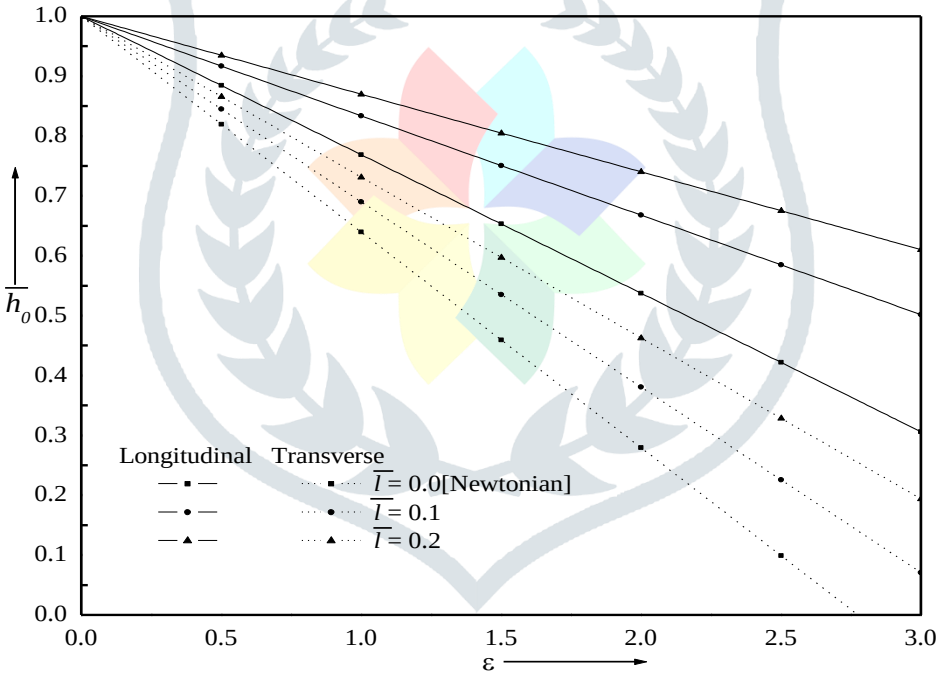

Fig.8. Variation of non-dimensional minimum film height $\overline{h}_0$ verses τ for different values of $\bar{l}$ with N = 0.8, ψ = 0.01, $\bar{c}$ = 0.2 and λ = 1.5

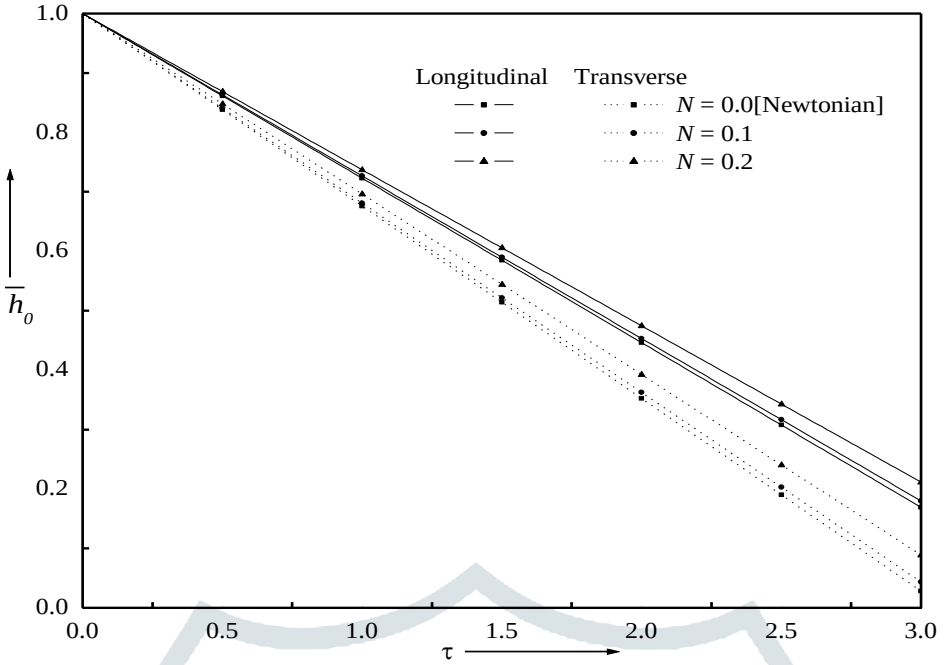

Fig.9. Variation of non-dimensional minimum film height $\overline{h_0}$ with τ for different values of N with $\overline{l}$ = 0.8, ψ = 0.1, $\overline{c}$ = 0.2 and λ = 2.5

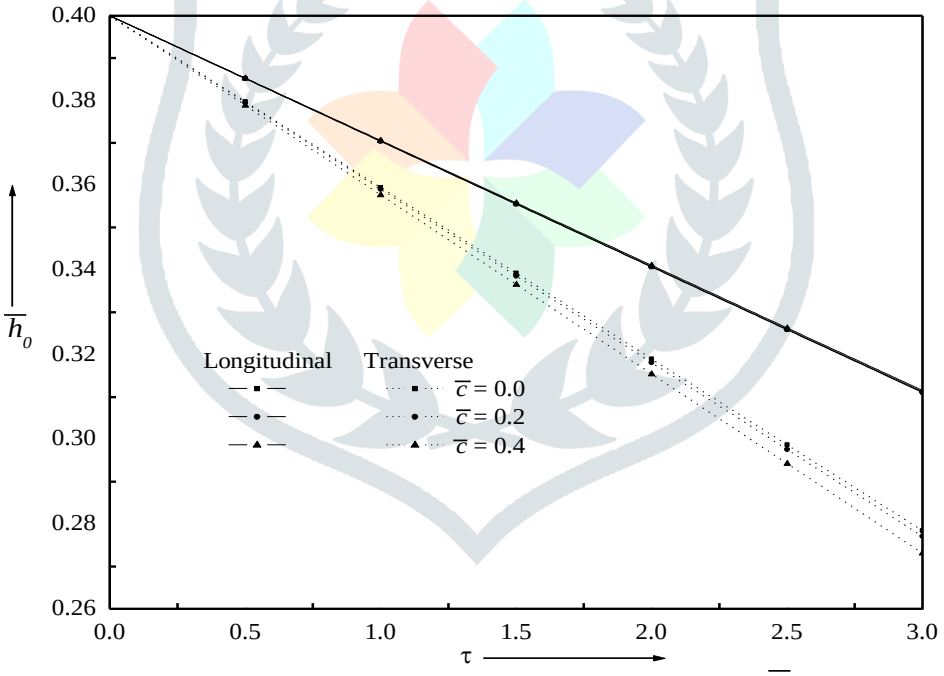

Fig.10. Variation of non-dimensional minimum film height $\overline{h_0}$ with τ for different values of $\overline{c}$ with N = 0.8, $\overline{l}$ = 0.2, ψ = 0.01 and λ = 3.0